Secondary processes driven by multi-factor interactions dominate the aerosol nitroaromatic compound pollution during winter in China

Yu Xu[1,2], Yu-Cheng You[1,2], Ting Yang[1,2], Lin Gui[1,2], Jun-Liang Tao[1,2], Tian-Shu Chen[1,2], Hao Xiao[1,2]*, Mei-Ju Yin[1,2], Hong-Wei Xiao[1,2], Hua-Yun Xiao[1,2]

[1]School of Agriculture and Biology, Shanghai Jiao Tong University, Shanghai 200240, China

[2]Shanghai Yangtze River Delta Eco-Environmental Change and Management Observation and Research Station (Shanghai Urban Ecosystem Research Station), Ministry of Science and Technology, National Forestry and Grassland Administration, 800 Dongchuan Rd., Shanghai 200240, China

*Corresponding authors

Hao Xiao

E-mail: xiaohao@sjtu.edu.cn

Phone: +86-152-7081-8726

Abstract: Previous observational and chamber studies have highlighted the significant promoting effects of relative humidity (RH) or aerosol liquid water (ALW) on the formation of aerosol NACs. However, the interpretability of this pattern needs further validation in large-scale field observations. This study presents the simultaneous investigation of the compositions, abundances, and potential origins of nitroaromatic compounds (NACs) in $PM_{2.5}$ across 11 Chinese cities during winter, with a focus on the key factors controlling their formation. Nitrophenols (NPs) and nitrocatechols (NCs) were identified as the main NAC groups, with their relative dominance varying by city. Higher total NAC concentrations were observed in northern cities, likely due to intensified biomass and coal combustion. While secondary processes dominated wintertime NAC formation across all investigated cities, the average proportion of secondarily formed NACs was lower in the north (87%) than in the south (93%). This north-south disparity was more pronounced during polluted periods (82% vs. 96%). Furthermore, insignificant promoting effect of RH or ALW was found for most NACs except nitrosalicylic acids. The constraining effects from O_3, ·OH, and solar radiation on NAC formation were stronger in northern China due to higher levels of light-absorbing air pollution (generally severer haze in the north), potentially offsetting the promoting effects of RH or ALW. These findings suggest that the RH- or ALW-promoted NAC formation may not be universally interpretable in real atmospheric environments, where multi-factor interactions play a critical role. This study highlights the necessity of considering complex field conditions in future research on NAC formation mechanisms.

1. Introduction

Nitrated phenol compounds are a class of aromatic organics characterized by the presence of both nitro (–NO_2) and hydroxyl (–OH) functional groups, which are ubiquitous in the atmospheric gas phase and particle phase (Cai et al., 2022; Li et al., 2020a; Huo et al., 2024). Key members of this nitroaromatic compound (NAC) class include nitrophenols, nitrocatechols, nitrosalicylic acids, nitroguaiacols, and their derivatives (Li et al., 2020c; Huang et al., 2024). NACs are important constituents of atmospheric fine particulate matter ($PM_{2.5}$) and are well recognized for their strong light-absorbing properties (Huang et al., 2025; Harrison et al., 2005; Wang et al., 2022). It has been reported that NAC species can contribute 4–50% or more to brown carbon light absorption (Mohr et al., 2013; Huang et al., 2024; Gu et al., 2022). Additionally, NACs are capable of strengthening the atmospheric oxidative capacity, as they promote the formation of HONO and OH radicals (·OH) (Selimovic et al., 2020; Yang et al., 2021). These distinctive physicochemical properties ultimately influence regional air quality, radiative forcing, and climate dynamics (Harrison et al., 2005; Xiong et al., 2025; Liu et al., 2023b). In particular, NACs can also pose health risks due to their potential mutagenic and cytotoxic properties(Harrison et al., 2005; Hao et al., 2020). Thus, elucidating the abundances and main sources of NACs in urban aerosol particles and the key factors driving their formation is essential for advancing effective air pollution prevention efforts.

The molecular composition of aerosol NACs and the relative abundance of individual NAC species are strongly influenced by a combination of primary emission

sources and secondary formation processes (Li et al., 2020b; Xie et al., 2019; Ma et al., 2024; Macfarlane et al., 2025; Wang et al., 2022). Extensive observational studies have confirmed that NACs in aerosols can originate from primary emissions such as coal combustion, biomass burning, and vehicle exhaust (Zhang et al., 2023; Ma et al., 2024; Macfarlane et al., 2025; Chen et al., 2022; Lu et al., 2019). Furthermore, NACs can be secondarily formed through gas-phase and liquid-phase oxidation of various precursors, such as toluene, benzene, xylene, phenol, catechol, m-cresol, guaiacol, and methyl catechol, in the presence of nitrogen oxides (NO_x), with their eventual distribution between gas and particle phases being significantly affected by gas-particle partitioning (Harrison et al., 2005; Wang and Li, 2021; Mayorga et al., 2021; Salvador et al., 2021; Vidović et al., 2019). Specifically, the formation of some NAC species in the particle phase involves nitration reactions of phenol, *o*-cresol, *o*-hydroxybenzoic acid, and *p*-hydroxybenzoic acid mediated by ·OH, NO_3·, NO_2·, N_2O_5, and $ClNO_2$ (Shi et al., 2023; Harrison et al., 2005; Wang and Li, 2021; Xiong et al., 2025). The atmospheric oxidation of catechol yields 4-nitrocatechol, a process initiated by ·OH and NO_3· (Finewax et al., 2018). Similarly, methylnitrophenol and methylnitrocatechol can be produced via the photooxidation of *m*-cresol followed by subsequent nitration (Olariu et al., 2002). These well documented pathways in both laboratory experiments and field observations facilitate the conversion of volatile organic compounds (VOCs) into NACs with relatively low volatility, thereby substantially contributing to the formation of secondary organic aerosols (SOA) (Harrison et al., 2005; Liu et al., 2023b; Kroflič et al., 2021; Finewax et al., 2018; Macfarlane et al., 2025). In particular, the formation

of NACs is influenced by variations in ambient conditions such as relative humidity (RH), aerosol liquid water (ALW) concentration, and temperature (Xiong et al., 2025; Liu et al., 2023b; Guo et al., 2024). Among these, RH and ALW represent the most widely reported atmospheric variables affecting NAC formation (Xiong et al., 2025; Liu et al., 2023b). Nevertheless, the underlying RH- and/or ALW-related mechanisms controlling NAC production remain highly complex and not yet fully elucidated.

It is generally accepted that an increase in RH can elevate the concentration of ALW (Xu et al., 2023; Xu et al., 2020b; Nguyen et al., 2016). ALW not only promotes the partitioning of water-soluble gaseous organics into the particle phase but also functions as a reaction medium for aqueous-phase processes, which significantly increase SOA production (Sareen et al., 2017; Yang et al., 2024; Ma et al., 2025; Xu et al., 2022; Liu et al., 2023a). Recently, smog chamber experiments have suggested a water cluster catalysis mechanism underlying NAC formation, in which gaseous water molecules form proton-transfer bridges, increasing the reaction rate constants for the H-shift by approximately 8 to 17 orders of magnitude at 298 K compared to the scenario with liquid water (Xiong et al., 2025). Additionally, previous field observations in cities such as Shanghai, Xi'an, and Beijing suggested that aerosol NAC levels did not exhibit a positive correlation with ALW (Huang et al., 2024; Liu et al., 2023b). Indeed, the mechanisms underlying the influence of RH and ALW on NAC formation remain a current research focus. However, to date, no large-scale synchronized observational studies in China have systematically investigated the linkages between aerosol NAC formation and RH or ALW.

Rapid urbanization and industrialization in China have intensified air pollution, especially during winter when biomass and coal combustion activities increase substantially (Ma et al., 2025; Xu et al., 2024b; Yang et al., 2025). Disparities in economic development levels among cities may consequently shape a unique spatial and temporal signature for NAC abundances, which are also modulated by factors like RH and ALW. In this study, we measured 9 typical NAC species in $PM_{2.5}$ samples simultaneously collected from 11 Chinese cities during winter. The objectives are: (1) to examine spatial variations in the concentration and composition of aerosol NACs; (2) to evaluate the relative contributions of primary emissions and secondary formation processes to aerosol NACs; and (3) to identify key factors governing the formation of NACs, with particular focus on the relationships between NAC abundances and RH and ALW levels in northern and southern China.

2. Materials and methods

2.1. Sampling sites and sample collection

The $PM_{2.5}$ sampling was conducted across 11 cities in China, geographically categorized into southern and northern groups based on the Qinling–Huaihe climatic boundary (**Figure S1**). The southern group consists of Guangzhou (GZ), Chengdu (CD), Guiyang (GY), Kunming (KM), Wuhan (WH), and Hangzhou (HZ). The northern sites encompass Lanzhou (LZ), Xi'an (XA), Beijing (BJ), Harbin (i.e., Haerbin; HEB), and Taiyuan (TY). Detailed information on all study sites was shown in **Sect. S1 in the Supplement**. The sampling campaign was carried out from December 10, 2017 to

January 14, 2018. A striking north-south temperature discrepancy was observed during this period. Specifically, the average ambient air temperature remained above 4°C in all southern cities, whereas it was generally below 2°C across the northern cities (**Tables S1**–**S4**). It is noteworthy that biomass and coal combustion activities are prevalent during winter in both southern and northern Chinese cities (Yang et al., 2025; Huang et al., 2024). However, as winters are typically colder in northern China, the demand for fossil fuels for heating is significantly higher there than in the south. For instance, the centralized winter heating policy in China is generally implemented only in northern regions during the cold season.

$PM_{2.5}$ samples were acquired using a high-volume air sampler (KC-1000, Laoying, China) operated at a constant flow rate of ~1.05 ± 0.03 m^3 min^{-1} at all study sites, with prebaked quartz fiber filters (Pallflex, Pall Corporation, USA) serving as the collection medium. Sampling was conducted simultaneously across 11 observation sites on a 2- to 3-day frequency cycle, with each sampling event lasting approximately 24 hours. Two field blank samples were prepared at each site by mounting filters in an identical but non-operating air sampler. This campaign yielded a total of 154 filter samples, which were subsequently preserved at –30 °C. Concurrent meteorological data (e.g., temperature and RH) and air pollutant concentrations (e.g., $PM_{2.5}$, SO_2, NO_x, CO, and O_3) recorded during the sampling dates were obtained from nearby monitoring stations. The solar shortwave radiation (SR) data were obtained from National Meteorological Information Center, China Meteorological Administration (http://data.cma.cn/). In addition, a $PM_{2.5}$ concentration threshold of 75 μg m^{-3} was applied to differentiate

between clean and polluted days throughout the sampling campaign (Xu et al., 2024b; Zhang and Cao, 2015). It should be noted that the $PM_{2.5}$ mass concentrations presented in this study represent regional average levels, rather than the actual values measured from the individual collected samples.

2.2. Chemical analysis and parameter calculation

The protocol for extracting NACs from filter samples followed an optimized sample preparation workflow (Frka et al., 2022; Huang et al., 2024; Ma et al., 2024; Ma et al., 2025). Briefly, a 10 cm^2 section of the filter was cut. The extraction was performed by sonicating the filter piece in 3 mL of methanol in an ice bath for 30 min, and this procedure was repeated twice. The extracts were then filtered through a 0.22 μm polytetrafluoroethylene syringe filter (CNW Technologies GmbH). The filtrate was concentrated under a gentle stream of nitrogen and adjusted with methanol containing 2,4,6-trinitrophenol to a final volume of 300 μL. After homogenization and centrifugation, the supernatant was analyzed using an Acquity ultrahigh-performance liquid chromatography (UPLC; Waters, USA) system coupled to a Xevo G2-XS Quadrupole time-of-flight mass spectrometer (ToF-MS; Waters, USA). The mass spectrometer was equipped with an electrospray ionization (ESI) source operated in negative ion mode. An ACQUITY UPLC HSS T3 column (2.1 mm × 100 mm, 1.8 μm; Waters, USA) was used for reversed-phase liquid chromatographic separation.

Nine NAC species were targeted for quantification, including 4-nitrophenol (4NP), 2,4-dinitrophenol (2,4DNP), 3-methyl-4-nitrophenol (3M4NP), 2-methyl-4-

nitrophenol (2M4NP), 4nitrocatechol (4NC), 4-methyl-5-nitrocatechol (4M5NC), 5-nitrosalicylic acid (5NSA), 3-nitro-salicylic acid (3NSA), and 4-nitroguaiacol (4NG). The recoveries of the standard reference materials varied between 94% and 105%, which is within the ranges reported in previous studies with UPLC-MS/MS-based NAC analysis (Frka et al., 2022; Huang et al., 2023; Kitanovski et al., 2012). The limits of detection and quantification ranged from 0.05 μg L^{-1} (for 5-nitrosalicylic acid) to 0.5 μg L^{-1} (for 4-nitroguaiacol) and from 0.15 μg L^{-1} (for 5-nitrosalicylic acid) to 1.5 μg L^{-1} (for 4-nitroguaiacol) for the target analytes, respectively. These values fell within the ranges established in previous UPLC-MS/MS methodology for NAC analysis (Frka et al., 2022; Huang et al., 2023; Li et al., 2020b). The repeatability for each standard, expressed as the relative standard deviation (n = 6), was less than 4.5%. None of these NACs were detectable in blank samples when analyzed using the identical measurement protocol. Furthermore, the UPLC-MS/MS analysis of these target NACs in atmospheric particles was found to be free of significant matrix effects (Kitanovski et al., 2012; Frka et al., 2022). In addition, two typical anthropogenic organosulfate markers (i.e., $C_8H_{17}O_4S^-$ and $C_5H_7O_6S^-$) were also measured via a comparable analytical approach (Yang et al., 2023; Xu et al., 2025; You et al., 2026). Detailed procedures for the identification and quantification of these organosulfate species have been described in our previous publications (Yang et al., 2023; Yang et al., 2024). Levoglucosan (LGA) was additionally identified based on a similar UPLC-MS method outlined above (Ma et al., 2025). In this study, the abundance of LGA was characterized by signal intensity.

The analytical procedure for inorganic ions in $PM_{2.5}$ samples involved the ultrapure water-based extraction via a ~4°C ultrasonic bath (Gui et al., 2025; Xu et al., 2024a). After extraction, the solutions were passed through a polytetrafluoroethylene syringe filter. Analysis was conducted via ion chromatography (Dionex ICS-5000+, Thermo Scientific, USA) to measure the concentrations of Mg^{2+}, Ca^{2+}, Na^{+}, Cl^{-}, SO_4^{2-}, NO_3^{-}, NH_4^{+}, and K^{+} (Xu et al., 2020a; Gui et al., 2024). The concentration of ALW and the pH value were estimated by running the ISORROPIA-II thermodynamic model in forward mode under the assumption of a metastable state (**Sect. S2 in the Supplement**), following methodologies well-documented in our previous work (Yang et al., 2024; Ma et al., 2025; Gui et al., 2025). In addition, the non-sea-salt fractions of K^{+} (nss-K^{+}) and Cl^{-} (nss-Cl^{-}) were derived by subtracting 0.038 and 1.727 times the Na^{+} concentration from the total concentration of each respective ion (Boreddy and Kawamura, 2015; Morales et al., 1998). The levels of ambient ·OH were estimated using the empirical formula proposed by Ehhalt and Rohrer (2000) (**Sect. S3 in the Supplement**), which was also detailed in our previous publications (Liu et al., 2023a; Xu et al., 2024a; Yin et al., 2026).

3. Results and discussion

3.1. Spatial characteristics of NAC concentration and composition in $PM_{2.5}$

Figure 1a–d shows the average concentration distributions of different NAC groups in $PM_{2.5}$ samples collected from 11 cities across China, along with a comparative analysis of their levels in southern and northern cities. NACs are categorized into four

groups, including nitrophenols (NPs), nitrocatechols (NCs), nitrosalicylic acids (NSAs), and nitroguaiacols (NGs) (**Table S1–S4**). On average, nitrophenols and nitrocatechols are the two dominant categories, constituting approximately 43.75 ± 14.33% and 42.44 ± 13.46% of the total measured NACs in the investigated cities, respectively (**Figure S2** and **Table S1–S2**). Nitrosalicylic acids and nitroguaiacols represent relatively minor proportions, account for only 6.12 ± 2.99% and 7.69 ± 1.80% of the total NACs, respectively. The highest average concentration of total nitrophenols was observed in TY, while the peak average level of total nitrocatechols was recorded in HEB. The lowest average total nitrophenol concentration was found in GZ, whereas HZ exhibited the lowest average total nitrocatechol level. Similarly, the average total abundances of nitrosalicylic acids and nitroguaiacils also showed significant spatial variations, with the highest mean values recorded in XA and HEB, respectively, and the lowest mean values in KM and HZ, respectively. Although neither nitrophenols nor nitrocatechols reached their individual peak concentrations in XA, the average total NAC concentration was the highest in this city (**Figure 1e** and **Table S1–S2**). Across all the investigated cities, the average concentration of total NACs was 20.09 ng m^{-3}, ranging from 5.55 ng m^{-3} to 44.87 ng m^{-3}. This falls within the range reported in previous studies (Huang et al., 2024; Liu et al., 2023b; Gu et al., 2022; Cai et al., 2022; Li et al., 2016). The second-highest total average NACs concentration was observed in HEB, followed by TY, XA, LZ, CD, BJ, GY, WH, HZ, KM, and GZ. For all four categories of NACs as well as the total NAC concentration, their average levels were consistently higher in northern cities than in southern cities (**Figure 1a-d** and **Figure S3**). This

spatial pattern is similar to that of $PM_{2.5}$ and SO_2 (typical pollutants emitted from coal combustion) (**Figure 1f,g**). Many previous studies have documented that the abundance of NACs in winter aerosols can be significantly influenced by primary emissions such as coal and biomass burning (Wang et al., 2017; Wang et al., 2020; Huang et al., 2023). Thus, the north-south gradient in NAC concentrations is likely closely associated with divergent air pollution levels (as indicated by $PM_{2.5}$ levels) between northern and southern China, partly driven by differences in coal combustion and biomass burning intensity.

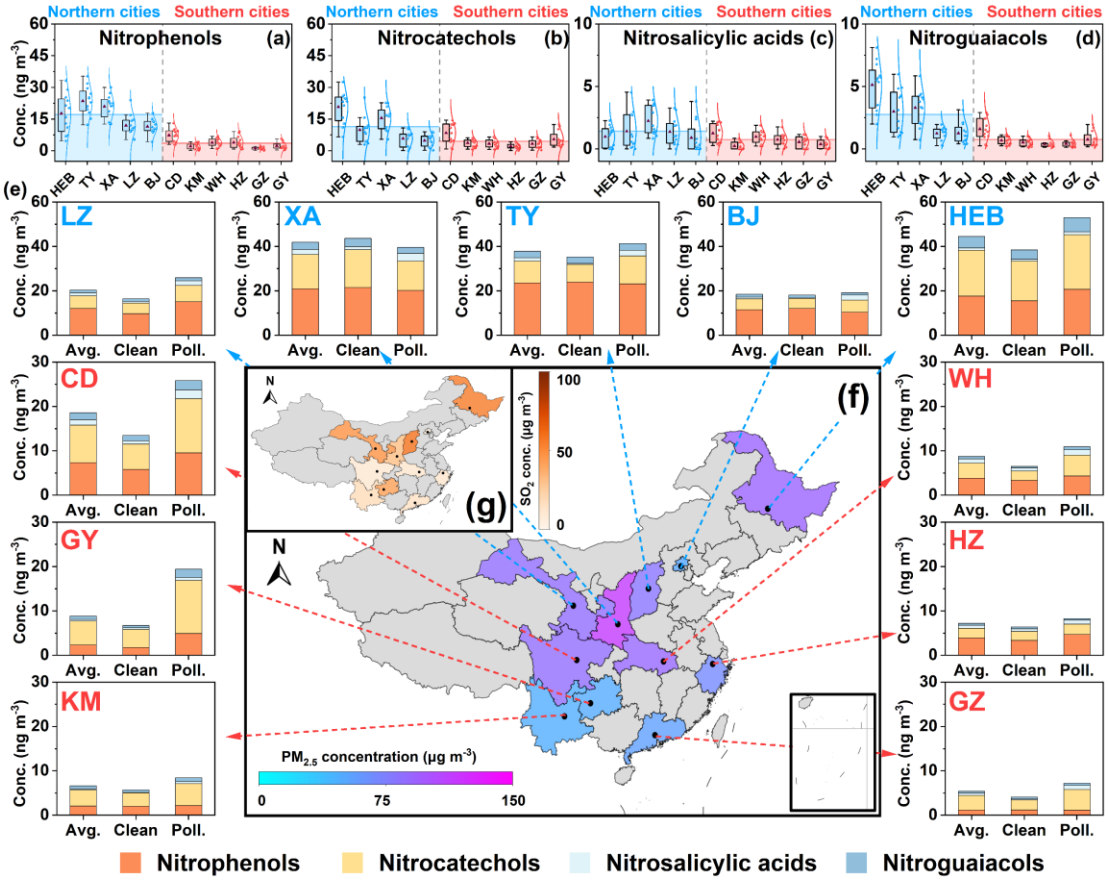

Figure 1. Box and whisker plots (a-d) showing the variations in the mean concentrations of different NAC groups in $PM_{2.5}$ collected in 11 Chinese cities. The

boxes represent the interquartile range (25th to 75th percentiles). The whiskers extend from the 5th to the 95th percentiles. The solid triangles inside boxes indicate the mean. (e) Average concentration distributions of detected NACs in $PM_{2.5}$ during clean and polluted days in winter across 11 Chinese cities. The color blocks in the panels (f) and (g) represent the spatial variations in $PM_{2.5}$ and SO_2 pollution levels, respectively, across the sampled cities during the study period. The map was obtained from ©MeteoInfoMap (Chinese Academy of Meteorological Sciences, China).

Among nitrophenols, 4-nitrophenol (4NP) was the most abundant species, accounting for 63.21 ± 8.07% of the total measured nitrophenols in China during winter (**Figure S4** and **Table S1–S4**). Previous studies characterizing NACs in biomass burning emissions have reported 4NP as an important emitted species (Huang et al., 2024; Wang et al., 2020; Wang et al., 2017). 4-nitrocatechol (4NC) was the dominant species among nitrocatechols. The average concentration of 4NC across all cities was 7.55 ± 6.90 ng m^{-3}, representing 40.67 ± 12.89 % of total NACs. The emission factors for 4NC from coal combustion varied widely based on geological maturity, ranging from 8 to 3487 μg kg^{-1} (Huang et al., 2023). In contrast, the emission factors of 4NP from the same coal sources were significantly lower, generally below 14 μg kg^{-1} (Huang et al., 2023). The average emission factor for nitrocatechols from the combustion of biomass materials was also substantial, measured at 26.6 ± 5.40 μg kg^{-1} (Huang et al., 2023). These findings indicate that coal and biomass burning during winter may significantly contribute to the abundance of NACs in urban aerosols across China,

273 particularly exacerbating NACs pollution in northern cities. Furthermore, we observed
274 that the 4M5NC concentrations measured in this study were lower than those reported
275 in several previous studies conducted in winter across urban China. For example, Wang
276 et al. (2019) measured a mean 4M5NC concentration of 0.56 ± 0.40 ng m^{-3} in winter
277 $PM_{2.5}$ from urban BJ, while Li et al. (2020b) reported a substantially higher mean
278 4M5NC value of 6.50 ± 6.38 ng m^{-3} for wintertime urban BJ. Huang et al. (2024) further
279 reported that mean 4M5NC concentrations in winter $PM_{2.5}$ across urban China varied
280 from 0.52 ± 0.53 ng m^{-3} (BJ) to 14.97 ± 9.23 ng m^{-3} (HEB). For Shanghai, Liu et al.
281 (2023b) observed a wintertime 4M5NC concentration of 0.11 ± 0.15 ng m^{-3} in $PM_{2.5}$ in
282 suburban areas, whereas Cai et al. (2022) reported a much higher concentration of 1.32
283 ± 1.14 ng m^{-3} in winter $PM_{2.5}$ at an urban site surrounded by multiple major traffic
284 arterial roads. These results suggest that 4M5NC concentrations in winter $PM_{2.5}$ vary
285 widely even within the same city. This variation is expected to be largely dependent on
286 sampling location and meteorological conditions. Presumably, the relatively low
287 4M5NC levels in this study may be partly attributed to the absence of prominent local
288 pollution sources (especially traffic emissions) near all sampling sites.

289 The mass concentration fractions of various NACs were further compared between
290 clean and polluted days (**Figure 1e**). It was observed that the dominant NAC groups
291 (i.e., nitrophenols and nitrocatechols) in $PM_{2.5}$ remained consistently predominant
292 across all cities from clean to polluted periods, without being superseded by other NAC
293 species. This pattern suggests that the main emission sources of aerosol NACs in these
294 urban areas may not have undergone significant changes during pollution periods. In

most cities, including LZ, HEB, CD, WH, GY, HZ, KM, and GZ, the average concentrations of total NACs and dominant NAC groups showed an increasing trend from clean to polluted periods (**Figure 1e** and **Table S1–S4**). In contrast, cities such as XA, TY, and BJ exhibited a decreasing trend in the concentrations of main NAC groups (i.e., nitrophenols). It should be noted that nitrophenols were not the primary species in GZ, and their average concentrations did not show an increasing trend from clean to polluted periods. As important contributors to haze formation, NACs would be expected to accumulate under polluted air conditions. Thus, the observed decrease in the abundance of some NAC groups on polluted days (typically associated with calm and stable weather conditions) in several cites suggests that the formation of NAC compounds may also be constrained by specific factors such as photolysis process (Liu et al., 2024; Yang et al., 2021), varied RH and ALW levels (Xiong et al., 2025; Liu et al., 2023b), and unfavorable atmospheric oxidation capacity (Wang and Li, 2021). These influencing factors will be further discussed in later sections. In general, the concentration and composition of NACs varied spatially (**Figure 1** and **Figure S2**), which may be attributed to spatial differences in precursor sources, emission intensities, and the key factors influencing aerosol NAC formation.

3.2. Temporal variations of NACs and their potential origins

Figure 2 shows the time series of concentrations of various NACs and key chemical components in winter $PM_{2.5}$ across northern and southern China. In northern China, the highest total NP concentration was observed in TY, whereas the highest total

NC concentration occurred in HEB (**Figure 2a,c,e**). In HEB, XA, and BJ, total NPs and total NCs exhibited similar variation trends (linear regression, $P < 0.05$), implying potentially similar sources for aerosol NPs and NCs. In TY and LZ, total NPs and total NCs also showed consistent variation patterns during most observation periods. Furthermore, NGs were significantly ($P < 0.05$) correlated with total NCs in all regions except TY and LZ. In southern cities, the most severe NACs pollution events were recorded in CD (**Figure 2b,d,f**), which may be attributed to the city's basin topography that hinders pollutant dispersion (Liao et al., 2017). With the exception of GZ, major NAC species in southern cities exhibited similar temporal trends. In GZ, several anomalously high NC cases likely led to inconsistent variation patterns among different NAC groups. Overall, the temporal variation trends of major NAC groups at the same site were highly consistent across most Chinese cities, indicating that the sources of different NACs during winter may be similar in each city.

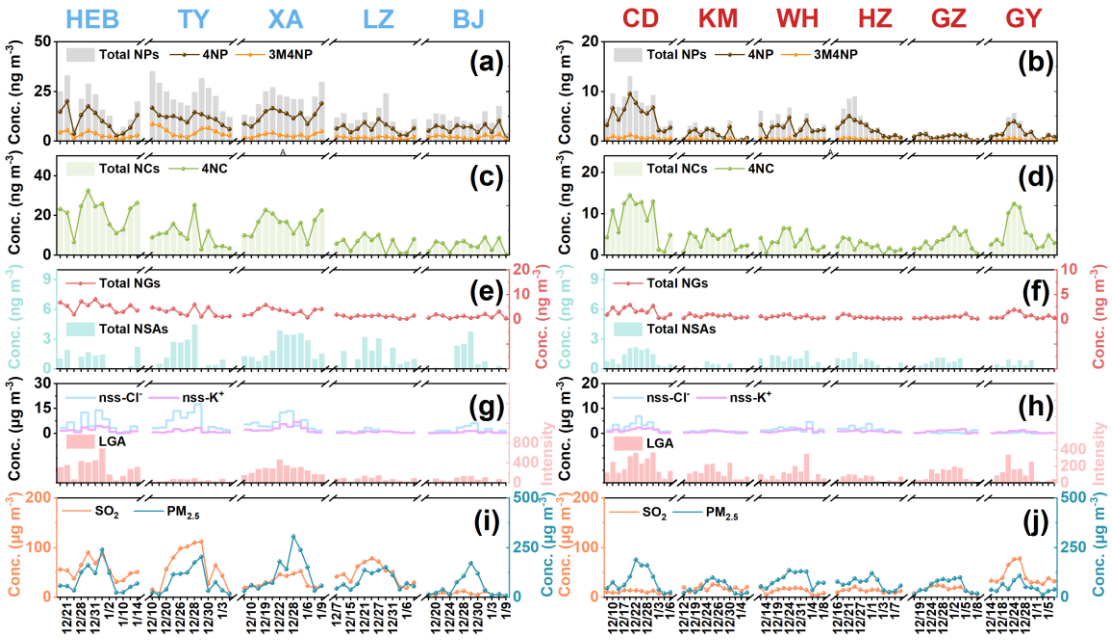

Figure 2. Temporal variations in (a–f) various NAC species and (g–l) key parameters in 11 Chinese cities.

Comparison of the temporal variation patterns (**Figure 2g–j**) and correlations of NACs against various combustion source tracers (**Figure 3a,b**) enabled the identification of their potential sources in the different cities (Huang et al., 2024; Cai et al., 2022; Wang et al., 2019; Kahnt et al., 2013). In northern cities, one or more NAC species showed consistent variation trends with indicators of biomass burning or coal combustion, including LGA, nss-K^+, SO_2, nss-Cl^-, and $C_8H_{17}O_4S^-$ (Kahnt et al., 2013; Ma et al., 2025; Yang et al., 2025; Yang et al., 2023) (**Figure 2g,i** and **Figure 3a**). The highest frequency of significant positive correlations between various NACs and biomass or coal combustion tracers (i.e., the number of orange-red rectangles marked with asterisks in the **Figure 3c**) was observed in HEB (n = 17), followed by LZ (n = 12), BJ (n = 10), TY (n = 7), and XA (n = 4). This suggests that the abundance of aerosol

NACs in northern cities was indeed significantly contributed by biomass and coal combustion. In most northern cities, the vehicle emission tracer $C_5H_7O_6S^-$ (Blair et al., 2017; Wang et al., 2021) showed insignificant positive correlation with NACs (**Figure 3a**). $C_5H_7O_6S^-$ only exhibited a significant positive correlation with NGs (a minor NACs component) in BJ. This suggests that the contribution of vehicle emissions to aerosol NACs in northern cities may be significantly smaller than that of biomass and coal combustion. However, this does not imply that the contribution of traffic-related precursors to secondary NACs was negligible, since only particulate-phase traffic tracers were employed in the analysis. In southern cities, the highest frequency of significant positive correlations between NACs and biomass burning or coal combustion tracers was found in KM (n = 22), followed by CD (n = 19), HZ (n = 15), GY (n = 10), WH (n = 10), and GZ (n = 5) (**Figure 3b, c**). Clearly, the frequency of significant positive correlations between NACs and biomass burning or coal combustion tracers was generally higher in southern China than in northern China (**Figure 3**). The result is fully consistent with the spatial distribution pattern shown in open fire spot maps, where southern China exhibited a higher density of fire spots compared to northern China (**Figure S5**). Importantly, although open fire spots are less frequent in the north, the colder climate there leads to widespread indoor use of biomass materials for heating and cooking in rural households, such as through traditional heated beds (kang). Thus, the above findings do not necessarily indicate that biomass burning released more NACs in southern China. In addition, the vehicle emission tracer $C_5H_7O_6S^-$ showed insignificant positive correlations with NACs in any southern cities

(**Figure 3b**). Given that NACs in the actual atmospheric environment are affected not only by primary emissions but also by secondary formation and removal processes, insignificant or weak correlations between various NACs and source-specific tracers do not necessarily indicate a lack of substantial influence from corresponding sources. However, the above correlation analysis can at least suggest that biomass and coal combustion play important roles in controlling aerosol NAC abundances in both northern and southern Chinese cities.

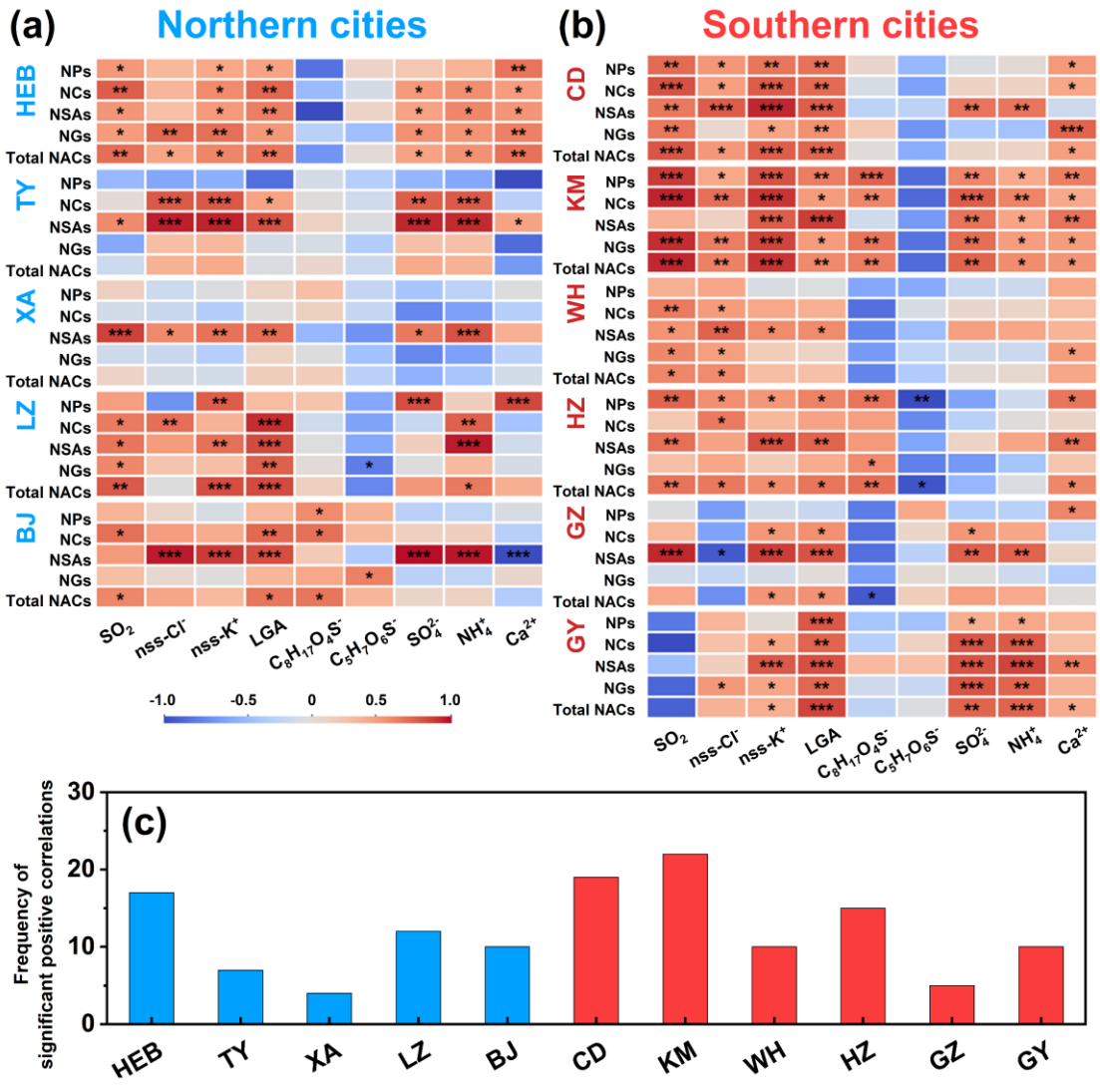

Figure 3. Correlations between various NAC species and indicative parameters in (a)

northern and (b) southern China. The colors of different solid rectangles indicate different correlation coefficients *r*. Symbols '***', '**', and '*' denote $P < 0.001$, $P < 0.01$, and $P < 0.05$, respectively. NACs are categorized into four groups, including nitrophenols (NPs), nitrocatechols (NCs), nitrosalicylic acids (NSAs), and nitroguaiacols (NGs). (c) Frequency of significant positive correlations between NACs and biomass burning or coal combustion tracers (i.e., the number of orange-red rectangles marked with asterisks in the panels a and b).

In addition, it is important to note that a critical distinction should be made regarding the role of biomass and coal combustion in shaping aerosol NAC composition and abundances. These combustion sources emit both primary NACs and volatile precursors that facilitate secondary NAC formation through atmospheric reactions. Thus, even though the correlation analysis mentioned above strongly implies biomass and coal combustion (typically considered primary sources) as significant contributors to NACs in winter aerosols in China, this evidence alone cannot attribute the NAC burden predominantly to direct primary emissions. The significant contributions may be also derived from efficient secondary formation processes initiated by the precursors co-emitted from these combustion activities.

3.3. Aerosol NACs dominated by secondary formation

To further determine the relative contributions of secondary oxidation processes and primary emissions to the measured aerosol NACs, an approach based on a tracer

species was employed (Salvador et al., 2021; Li et al., 2019). This method is similar to the elemental carbon-tracer technique utilized for estimating secondary organic carbon. Its specific application refers to the following equation 1 (Chen et al., 2022; Liu et al., 2023b; Cai et al., 2022).

$$[\mathrm{NACs}]_{\mathrm{sec.}} = [\mathrm{NACs}]_{\mathrm{total}} - \left(\frac{[\mathrm{NACs}]}{[\mathrm{Tracer}]}\right)_{\mathrm{pri.}} \times [\mathrm{Tracer}] \quad (1)$$

where $[\mathrm{NACs}]_{\mathrm{sec.}}$, $[\mathrm{NACs}]_{\mathrm{total}}$, and [Tracer] correspond to the concentrations of secondarily formed NACs, the total measured NACs, and the tracer, respectively. Carbon monoxide served as the indicator for combustion sources. The term $\left(\frac{[\mathrm{NACs}]}{[\mathrm{Tracer}]}\right)_{\mathrm{pri.}}$ represents the concentration ratio of NACs to carbon monoxide. This ratio was derived by fitting the lowest 15% of the observed $\left(\frac{[\mathrm{NACs}]}{[\mathrm{Tracer}]}\right)$ values, with the underlying assumption that these data reflect periods dominated by primary emissions (Chen et al., 2022). The 15% threshold was selected primarily to facilitate direct and consistent comparison with the results reported in previous studies (Liu et al., 2023b; Cai et al., 2022). Theoretically, the adoption of high-frequency measurement data in the above calculation can better capture the realistic fluctuations in the [NACs]/[Tracer] ratio. In both previous relevant studies (Liu et al., 2023b; Cai et al., 2022) and the present work, 12–24 h integrated observation data are commonly used for this calculation, and the resulting values largely reflect the regional average levels of secondary NACs. More importantly, given that the atmospheric lifetime of NACs is significantly shorter than that of tracer (i.e., CO), calculating the [NACs]/[Tracer] ratio using non-high-frequency data may lead to an underestimation of the actual [NACs]/[Tracer] ratio, which in turn causes an overestimation of the calculated secondary NAC fraction. Thus, the

secondary NAC values calculated in this study only represented the maximum average fractions of secondary NACs over the study period. These values were exclusively used for internal data comparison within this study, as well as for cross-comparison with results reported in previous studies that employed an analogous calculation method based on non-high-frequency observation data (Liu et al., 2023b; Cai et al., 2022).

Figure 4 and **Figure S6** show the contribution of secondarily formed NACs to the total measured NAC mass in $PM_{2.5}$ across 11 Chinese cities. In northern cities, the proportion of secondary NACs in the particle phase was highest in XA (92%), followed by HEB (91%), BJ (87%), LZ (83%), and TY (80%) (**Figure 4a** and **Table S5**). On average, the contribution of secondarily formed NACs to the total aerosol NAC mass in the investigated northern cities was 87%, which was slightly lower than that observed in the southern cities (93%) (**Figure 4b** and **Table S5**). Among the southern cities, the maximum and minimum average secondary NAC contributions to total aerosol NACs were observed in GZ (96%) and GY (88%), respectively. Overall, the secondary formation pathway dominated the total NAC masses in $PM_{2.5}$ during winter in Chinese cities. Similarly, an observational study on the secondary formation of brown carbon conducted in Chongming Island, Shanghai, also reported that the fraction of secondary NACs in $PM_{2.5}$ exceeded 80% during haze episodes (Liu et al., 2023b). Another study in urban Shanghai reported that secondary formation accounted for up to 75% of total aerosol NACs in winter $PM_{2.5}$ (Cai et al., 2022). These findings further corroborate the significance of secondary production in shaping aerosol NAC pollution during winter in Chinese cities.

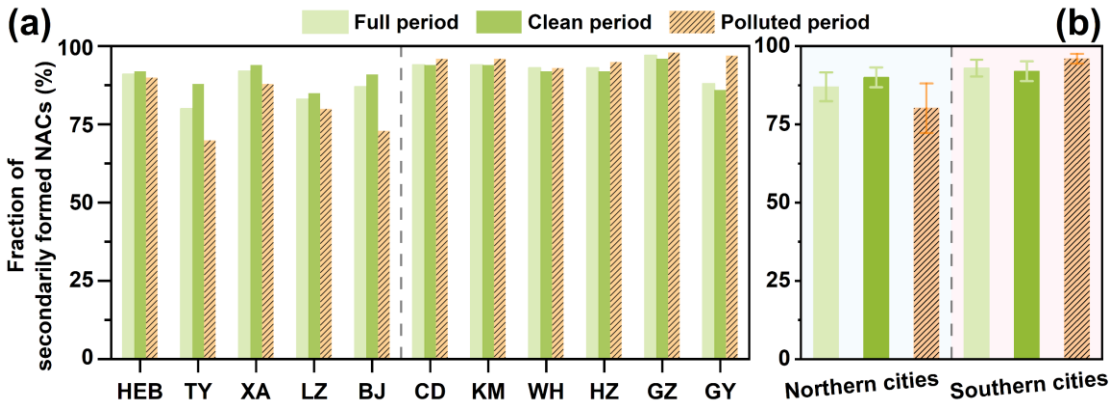

Figure 4. (a) Average contribution of secondarily formed NACs to the total measured NAC mass in $PM_{2.5}$ in different periods across 11 Chinese cities. (b) Average contribution of secondarily formed NACs to the total measured NAC mass in $PM_{2.5}$ in different periods in northern and southern China.

Furthermore, we observed a declining trend in the proportional contribution of secondarily formed NACs to total aerosol NACs from clean to polluted periods across all northern Chinese cities (**Figure 4**). This pattern suggests either an increased contribution from primary emission sources (e.g., biomass and coal combustion) to aerosol NACs, or the presence of limiting factors that suppress the yield of secondary NAC formation on polluted days. Biomass and coal combustion have been identified as significant primary sources of NACs during winter in China (**Figure 3**) (Salvador et al., 2021; Li et al., 2020a; Li et al., 2016); moreover, these anthropogenic activities occur regularly daily throughout the cold season. Thus, changing meteorological factors during polluted days (e.g., reduced planetary boundary layer height (PBLH) and weakened wind speed (**Tables S1–S4**)) may be important drivers of aerosol NAC

462 accumulation. Nevertheless, the fact that the fraction of secondary NACs decreased
463 during northern pollution episodes implies the existence of specific factors that
464 constrained secondary NAC yields under polluted conditions. In contrast, southern
465 cities exhibit an increasing trend in the relative abundance of secondary NACs from
466 clean to polluted periods. This pattern may be more intuitively explained, as elevated
467 ALW concentrations, lower PBLH, and increased NO_x levels during polluted episodes
468 can promote the secondary formation of NACs or the direct partitioning of gaseous
469 NACs into the particle phase. Overall, aerosol NACs in China during winter were
470 dominated by secondary processes; however, the complex factors regulating NAC
471 formation require further differentiation between northern and southern cities.
472
473 **3.4. Potential promotion and constraint effects on the formation of aerosol NACs**
474 The secondary formation of NACs proceeds via gas-phase photochemical
475 reactions and aqueous-phase processes within aerosols (Harrison et al., 2005; Yang et
476 al., 2020). For example, the gas-phase process often begins with the oxidation of
477 volatile aromatic precursors like benzene and toluene by ·OH, leading to the formation
478 of phenolic compounds (Chen et al., 2022). These phenols can further react with ·OH
479 during the day or with NO_3· at night, generating phenoxy radicals (Wang and Li, 2021;
480 Atkinson et al., 1992; Olariu et al., 2002; Olariu et al., 2013). The addition of NO_2 to
481 these radicals results in the formation of nitrophenols and nitrocatechols (Rana and
482 Guzman, 2022). Subsequently, these NACs can partition into the aqueous-phase in
483 aerosols. Simultaneously, phenolic compounds in aqueous-phase can also undergo

nitration (Vidović et al., 2018; Harrison et al., 2005). Thus, increased ALW levels are expected to promote the enrichment of NACs in aerosol particles. Conversely, photodegradation and enhanced atmospheric oxidation capacity can facilitate the removal of NACs. Recent field observations and chamber experiments have suggested a significant positive correlation between the concentration of particulate NACs and RH (Xiong et al., 2025); moreover, the authors proposed a previously overlooked but efficient NAC formation pathway driven by gaseous water clusters, in addition to the well-known ALW mediated processes (Xiong et al., 2025). Interestingly, recent simulations on nitrate-mediated aqueous-phase photooxidation of NACs have suggested that increasing aerosol nitrate concentrations can significantly enhance the photolysis rates of 4-nitrocatechol, 3-nitrosalicylic acid, and 3,4-dinitrophenol by 3 to 3.5 times compared to nitrate-free cases (Liu et al., 2025). Consequently, we further examined the correlations between the abundance of NACs and the key factors affecting their formation (e.g., ALW, RH, radiation intensity, atmospheric oxidation capacity, and nitrate levels) in field environments (**Figure 5**). This approach is commonly employed in observation studies to identify the critical factors affecting the concentrations of target compounds (Yang et al., 2020; Liu et al., 2023b; Huang et al., 2023; Liu et al., 2023a; Gui et al., 2025).

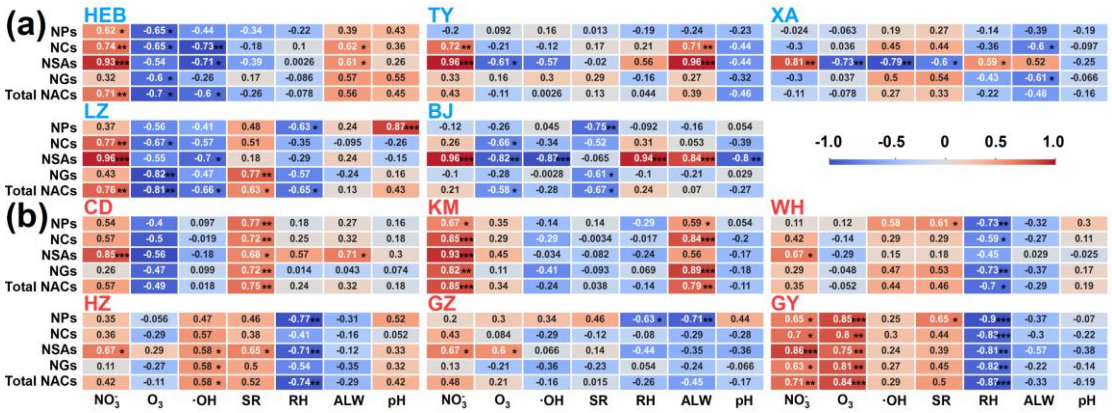

503

504 **Figure 5.** Correlations between various NAC species and factors potentially affecting
505 their formation in (a) northern and (b) southern China. The colors of different solid
506 rectangles indicate different correlation coefficients *r* (shown inside the rectangles).
507 Symbols '***', '**', and '*' denote $P < 0.001$, $P < 0.01$, and $P < 0.05$, respectively.

508

509 In most northern Chinese cities (e.g., HEB, TY, XA, and LZ), insignificant positive
510 correlations were observed between various NACs (except NSAs) and RH; instead,
511 negative correlations were identified between them (**Figure 5a**). In XA and BJ, only
512 NSAs show a significant positive correlation with RH. Similarly, a general negative
513 correlation trend between NACs and RH was prevalent in most southern cities (**Figure**
514 **5b**). These field observations clearly contrasted with recently reported laboratory
515 findings where RH was shown to significantly promote NAC formation. This indicates
516 that NAC formation in complex real-world environments may be co-controlled by
517 multiple factors. The correlation patterns between ALW and NACs were largely similar
518 to those of RH across most investigated Chinese cities. However, in TY and KM, ALW
519 showed significant positive correlations with NACs. Furthermore, we found that ALW
520 and RH levels were generally higher on polluted days compared to clean days across

521 the studied cities (**Figure S7** and **Tables S1–S4**). However, as discussed above, the
522 concentrations of major NAC species did not increase in some cities (**Figure 1**), further
523 implying that ALW and RH were not deterministic factors for NAC accumulation
524 during pollution episodes. Although a recent study conducted a laboratory located in
525 XA has suggested that increased aerosol nitrate can enhance NAC photolysis (Liu et al.,
526 2025), nitrate concentrations showed a positive correlation with NACs in most
527 investigated cities (except XA) (**Figure 5**). This suggests that in ambient environments,
528 the significant positive correlation between nitrate (a common transformation product
529 of combustion-derived NO_x) and NACs likely indicates that NAC formation was
530 closely linked to combustion emissions and NO_x-involved secondary chemistry. In
531 addition, atmospheric oxidants (e.g., O_3 and ·OH) and SR exhibited negative
532 correlations with NACs in most northern cities. In contrast, O_3, ·OH and SR exerted a
533 promoting effect on NAC formation in some southern cities such as CD, WH, HZ, and
534 GY. These distinctions underscore the necessity for region-specific assessment of NAC
535 formation mechanisms and their drivers.

536 To visually compare the key factors influencing the formation of aerosol NACs in
537 northern and southern China, we pooled data from all cities in these two regions to
538 perform Mantel test analysis and principal component analysis (PCA) (**Figure 6**). In
539 both southern and northern China, only NSAs exhibited a significant correlation with
540 ALW (**Figure 6a,b**). This is likely because the carboxyl group present in NSAs
541 promotes ionization in water, thereby enhancing their solubility. Although PCA results
542 indicate the homology of various NACs (excluding NSAs) (**Figure 6c,d**), the

significant promotional effects of RH and ALW on NCs, NPs, and NGs were not reflected in either the Mantel test or PCA analyses. Furthermore, in northern China, SR showed an opposite vector direction to NCs, NPs, and NGs in the PCA plot (**Figure 6c**), indicating a notable inhibitory effect of photodegradation on their accumulation in particles (Liu et al., 2024). During winter, the atmospheric fine particulate pollution was generally more severe in northern cities than in southern cities (**Figure 1f** and **Tables S1–S4**), and the abundance of NACs was also greater in the north (**Figure 1f** and **Figure S3**). These findings imply that the light absorption capacity of aerosols in northern cities were stronger that in southern cities (Huang et al., 2024). This may explain why NACs in northern cities showed a significant negative correlation with SR and why the proportion of secondarily formed NACs in the total measured NACs was lower in the north than in the south, especially during pollution episodes. Additionally, the constraining effect of O_3 or ·OH on NAC formation was greater in northern China (evidenced by larger angles between them in **Figure 6c**) than in southern China (**Figure 6d**). Similar conclusions can also be more intuitively obtained in the Mantel test analysis results (**Figure 6a,b**). Overall, our findings indicate that the promotional effects of RH and ALW on NAC formation were insignificant in field observation in China during winter. This could be attributed to the synergistic constraints of multiple factors, such as photolysis, O_3, and ·OH (**Figure 7**).

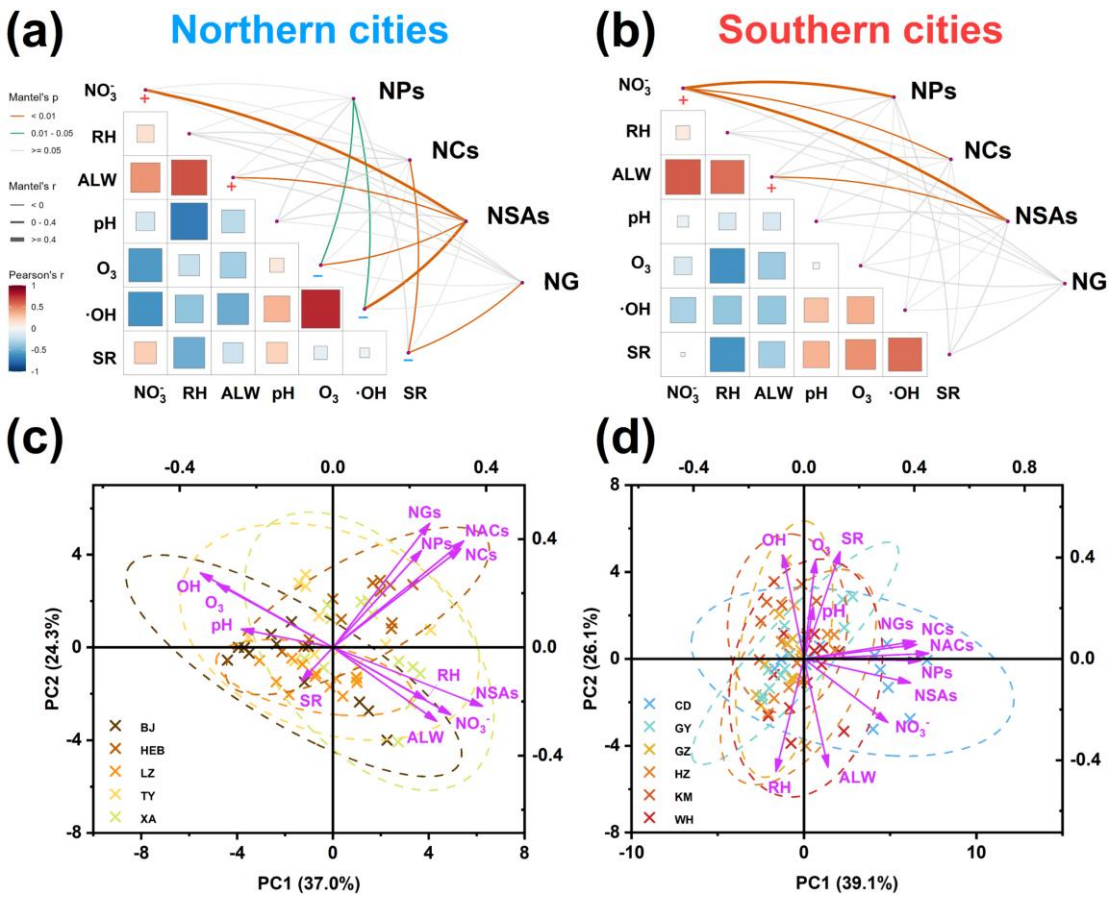

562 **Figure 6.** Mantel test correlation heatmap showing the interrelationships between
563 different factors or parameters for the pooled data from (a) northern and (b) southern
564 China. The size of the solid square indicates the significance of the correlation between
565 the two corresponding parameters. The larger square indicates that the correlation is
566 more significant. The colors of the different solid circles indicate different correlation
567 coefficients (*r*). The symbols '+' and '–' refer to positive and negative correlations,
568 respectively. Principal component analysis result deciphering the interrelationships
569 among different factors or parameters for the pooled data from (c) northern and (d)
570 southern China.

571

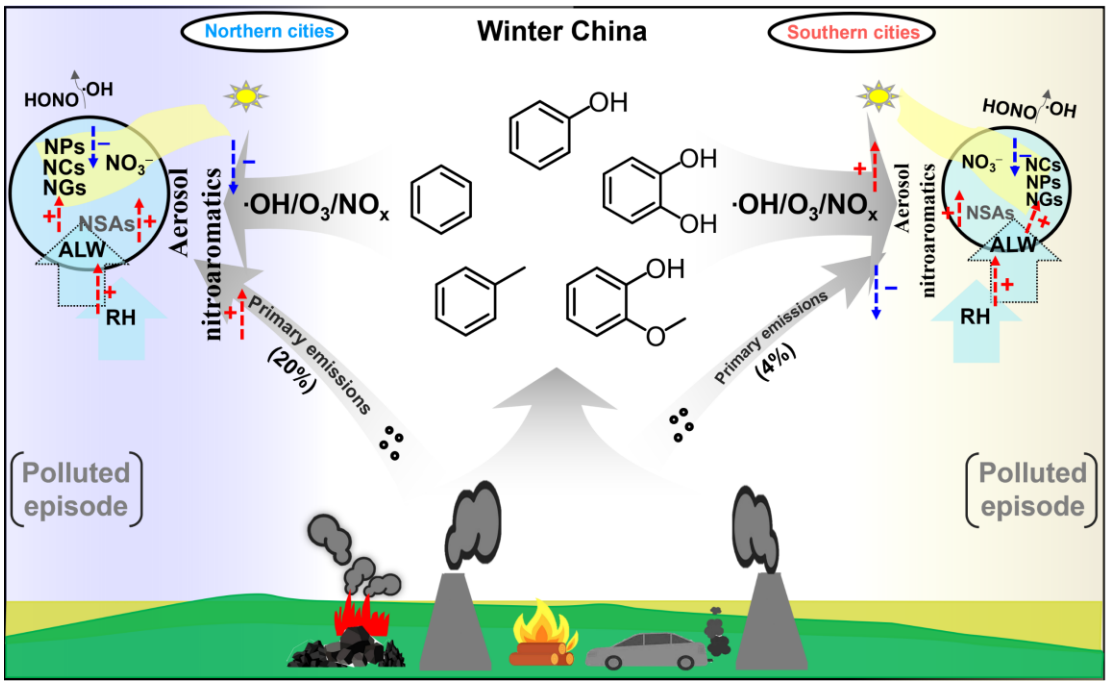

572 **Figure 7.** Conceptual illustration showing that the secondary processes driven by multi-
573 factor interactions modulate the aerosol NAC pollution during winter in southern and
574 northern China. The "+" and "–" symbols indicate promoting and constraining effects,
575 respectively.

576

577 **4. Conclusion and atmospheric implications**

578 To the best of our knowledge, this study presents the first simultaneous
579 investigation of the abundances, compositions, and potential origins of NACs in $PM_{2.5}$
580 across 11 Chinese cities during winter, along with the key factors controlling their
581 formation. On average, NPs and NCs were identified as the two predominant groups of
582 NACs. Their relative contributions to the total NAC abundance varied by city, with
583 either NPs or NCs being dominant depending on location. Overall, the abundance of
584 aerosol NACs was higher in northern China compared to southern China, likely
585 attributable to more intensive coal and biomass burning activities in the north.

Furthermore, we found that aerosol NACs in China during winter were predominantly formed via secondary processes. However, the proportion of secondarily formed NACs in the total measured NACs was lower in the north than in the south. This north-south difference was further amplified during polluted periods.

The significant promotional effects of RH and ALW on NCs, NPs, and NGs were not observed in either northern or southern China. Only NSAs showed a significant positive correlation with ALW across both regions. Furthermore, the constraining effects of O_3, ·OH, or SR on NAC formation were more pronounced in northern China compared to southern China. This may have attenuated the promotional effects of RH and ALW on NAC formation (**Figure 7**). Previous observational and simulation studies have emphasized the significant promotional role of RH and/or ALW in the formation of aerosol nitrogen-containing organic compounds (including NACs) (Xiong et al., 2025; Xu et al., 2020b; Ma et al., 2025). However, this large-scale observational study suggests that the generalizability of such RH- and ALW-regulated promotional effects on NAC formation in real atmospheric environments requires further validation. We acknowledge that individual factors (e.g., RH or ALW) play a crucial role in governing aerosol NAC formation. Nevertheless, field environments are often more complex than laboratory-simulated scenarios. Thus, the overall results highlight that future investigations into NAC formation mechanisms should consider the impacts of multi-factor interactions.

Data availability. The data presented in this work are available upon request from the

first author or corresponding author.

Author contributions. HYX, HX, and YX designed the study; YX, YCY, TY, LG, JLT, TSC, HWX, and HX performed field measurements and sample collection; TY and YCY performed chemical analysis; YX and YCY performed data analysis; YX wrote the original manuscript; and HYX, HX, and YX reviewed and edited the manuscript.

Financial support. This study was kindly supported by Key Program of the National Natural Science Foundation of China (grant number 42430501), National Natural Science Foundation of China (grant number 42303081 and 42403077), Science and Technology Innovation Program of Hunan Province (grant number 2025AQ2001), and National Key Research and Development Program of China (grant number 2023YFF0806001).

Conflict of Interest. The authors declare no conflicts of interest relevant to this study.

References

Atkinson, R., Aschmann, S. M., and Arey, J.: Reactions of hydroxyl and nitrogen trioxide radicals with phenol, cresols, and 2-nitrophenol at 296 .+-. 2 K, Environ. Sci. Technol., 26, 1397-1403, 10.1021/es00031a018, 1992.

Blair, S. L., MacMillan, A. C., Drozd, G. T., Goldstein, A. H., Chu, R. K., Paša-Tolić, L., Shaw, J. B., Tolić, N., Lin, P., Laskin, J., Laskin, A., and Nizkorodov, S. A.: Molecular Characterization of Organosulfur Compounds in Biodiesel and Diesel Fuel Secondary Organic Aerosol, Environ. Sci. Technol., 51, 119-127, 10.1021/acs.est.6b03304, 2017.

Boreddy, S. K. R. and Kawamura, K.: A 12-year observation of water-soluble ions in TSP aerosols collected at a remote marine location in the western North Pacific: an outflow region of Asian dust, Atmos. Chem. Phys., 15, 6437-6453, 10.5194/acp-15-6437-2015, 2015.

Cai, D., Wang, X., George, C., Cheng, T., Herrmann, H., Li, X., and Chen, J.: Formation of Secondary Nitroaromatic Compounds in Polluted Urban Environments, J. Geophys. Res.: Atmos., 127, e2021JD036167, https://doi.org/10.1029/2021JD036167, 2022.

Chen, Y., Zheng, P., Wang, Z., Pu, W., Tan, Y., Yu, C., Xia, M., Wang, W., Guo, J., Huang, D., Yan, C., Nie, W., Ling, Z., Chen, Q., Lee, S., and Wang, T.: Secondary Formation and Impacts of Gaseous Nitro-Phenolic Compounds in the Continental Outflow Observed at a Background Site in South China, Environ. Sci. Technol., 56, 6933-6943, 10.1021/acs.est.1c04596, 2022.

Ehhalt, D. H. and Rohrer, F.: Dependence of the OH concentration on solar UV, J. Geophys. Res.: Atmos., 105, 3565-3571, 10.1029/1999jd901070, 2000.

Finewax, Z., de Gouw, J. A., and Ziemann, P. J.: Identification and Quantification of 4-Nitrocatechol Formed from OH and NO3 Radical-Initiated Reactions of Catechol in Air in the Presence of NOx: Implications for Secondary Organic Aerosol Formation from Biomass Burning, Environ. Sci. Technol., 52, 1981-1989, 10.1021/acs.est.7b05864, 2018.

Frka, S., Šala, M., Brodnik, H., Štefane, B., Kroflič, A., and Grgić, I.: Seasonal variability of nitroaromatic compounds in ambient aerosols: Mass size distribution, possible sources and contribution to water-soluble brown carbon light absorption, Chemosphere, 299, 134381, https://doi.org/10.1016/j.chemosphere.2022.134381, 2022.

Gu, C., Cui, S., Ge, X., Wang, Z., Chen, M., Qian, Z., Liu, Z., Wang, X., and Zhang, Y.: Chemical

654 composition, sources and optical properties of nitrated aromatic compounds in fine particulate matter
655 during winter foggy days in Nanjing, China, Environ. Res., 212, 113255,
656 https://doi.org/10.1016/j.envres.2022.113255, 2022.
657 Gui, L., Xu, Y., Ma, Y.-J., Yang, T., Xiao, H.-W., Xiao, H., and Xiao, H.-Y.: Firework Display Is a
658 Newly Identified Source of Gaseous and Particulate Amines, Environ. Sci. Technol. Lett., 12, 1387-1393,
659 10.1021/acs.estlett.5c00806, 2025.
660 Gui, L., Xu, Y., You, Y.-C., Ma, Y.-J., Yang, T., Liu, T., Xiao, H.-W., Xiao, H., and Xiao, H.-Y.:
661 Oxidative Degradation of Higher-Molecular-Weight Aromatic Amine Compounds Is a Potential Source
662 of Anilinium in Urban Aerosols, Environ. Sci. Technol. Lett., 11, 1355−1361,
663 10.1021/acs.estlett.4c00935, 2024.
664 Guo, Z., Hu, X., Sun, W., Peng, X., Fu, Y., Liu, K., Liu, F., Meng, H., Zhu, Y., Zhang, G., Wang, X.,
665 Xue, L., Wang, J., Wang, X., Peng, P. a., and Bi, X.: Mixing state and influence factors controlling diurnal
666 variation of particulate nitrophenol compounds at a suburban area in northern China, Environ. Pollut.,
667 344, 123368, https://doi.org/10.1016/j.envpol.2024.123368, 2024.
668 Hao, Y., Sun, G., Fan, T., Tang, X., Zhang, J., Liu, Y., Zhang, N., Zhao, L., Zhong, R., and Peng, Y.:
669 In vivo toxicity of nitroaromatic compounds to rats: QSTR modelling and interspecies toxicity
670 relationship with mouse, J. Hazard. Mater., 399, 122981, https://doi.org/10.1016/j.jhazmat.2020.122981,
671 2020.
672 Harrison, M. A. J., Barra, S., Borghesi, D., Vione, D., Arsene, C., and Iulian Olariu, R.: Nitrated
673 phenols in the atmosphere: a review, Atmos. Environ., 39, 231-248,
674 https://doi.org/10.1016/j.atmosenv.2004.09.044, 2005.
675 Huang, S., Shen, Z., Bai, G., Zhang, L., Wang, D., Li, C., Zheng, H., Xu, H., and Zhang, Y.:
676 Photochemical Aging of PM2.5 Nitroaromatic Compounds From Solid Fuel Combustion Enhanced Light
677 Absorption and Oxidation Potential, J. Geophys. Res.: Atmos., 130, e2025JD043471,
678 https://doi.org/10.1029/2025JD043471, 2025.
679 Huang, S., Yang, X., Xu, H., Zeng, Y., Li, D., Sun, J., Ho, S. S. H., Zhang, Y., Cao, J., and Shen, Z.:
680 Insights into the nitroaromatic compounds, formation, and light absorption contributing emissions from
681 various geological maturity coals, Sci. Total Environ., 870, 162033,
682 https://doi.org/10.1016/j.scitotenv.2023.162033, 2023.

683 Huang, S., Shen, Z., Yang, X., Bai, G., Zhang, L., Zeng, Y., Sun, J., Xu, H., Ho, S. S. H., Zhang, Y.,
684 and Cao, J.: Nitroaromatic compounds in six major Chinese cities: Influence of different formation
685 mechanisms on light absorption properties, Sci. Total Environ., 930, 172672,
686 https://doi.org/10.1016/j.scitotenv.2024.172672, 2024.
687 Huo, Y., Li, M., Wang, X., Sun, J., Zhou, Y., Ma, Y., and He, M.: Rapid oxidation of phenolic
688 compounds by O3 and HO: effects of the air–water interface and mineral dust in tropospheric chemical
689 processes, Atmos. Chem. Phys., 24, 12409-12423, 10.5194/acp-24-12409-2024, 2024.
690 Kahnt, A., Behrouzi, S., Vermeylen, R., Safi Shalamzari, M., Vercauteren, J., Roekens, E., Claeys,
691 M., and Maenhaut, W.: One-year study of nitro-organic compounds and their relation to wood burning
692 in PM10 aerosol from a rural site in Belgium, Atmos. Environ., 81, 561-568,
693 https://doi.org/10.1016/j.atmosenv.2013.09.041, 2013.
694 Kitanovski, Z., Grgić, I., Vermeylen, R., Claeys, M., and Maenhaut, W.: Liquid chromatography
695 tandem mass spectrometry method for characterization of monoaromatic nitro-compounds in
696 atmospheric particulate matter, J. Chromatogr. A, 1268, 35-43,
697 https://doi.org/10.1016/j.chroma.2012.10.021, 2012.
698 Kroflič, A., Anders, J., Drventić, I., Mettke, P., Böge, O., Mutzel, A., Kleffmann, J., and Herrmann,
699 H.: Guaiacol Nitration in a Simulated Atmospheric Aerosol with an Emphasis on Atmospheric
700 Nitrophenol Formation Mechanisms, ACS Earth Space Chem., 5, 1083-1093,
701 10.1021/acsearthspacechem.1c00014, 2021.
702 Li, K., Li, J., Tong, S., Wang, W., Huang, R. J., and Ge, M.: Characteristics of wintertime VOCs in
703 suburban and urban Beijing: concentrations, emission ratios, and festival effects, Atmos. Chem. Phys.,
704 19, 8021-8036, 10.5194/acp-19-8021-2019, 2019.
705 Li, M., Wang, X., Lu, C., Li, R., Zhang, J., Dong, S., Yang, L., Xue, L., Chen, J., and Wang, W.:
706 Nitrated phenols and the phenolic precursors in the atmosphere in urban Jinan, China, Sci. Total Environ.,
707 714, 136760, https://doi.org/10.1016/j.scitotenv.2020.136760, 2020a.
708 Li, X., Yang, Y., Liu, S., Zhao, Q., Wang, G., and Wang, Y.: Light absorption properties of brown
709 carbon (BrC) in autumn and winter in Beijing: Composition, formation and contribution of nitrated
710 aromatic compounds, Atmos. Environ., 223, 117289, https://doi.org/10.1016/j.atmosenv.2020.117289,
711 2020b.

712 Li, X., Wang, Y., Hu, M., Tan, T., Li, M., Wu, Z., Chen, S., and Tang, X.: Characterizing chemical
713 composition and light absorption of nitroaromatic compounds in the winter of Beijing, Atmos. Environ.,
714 237, 117712, https://doi.org/10.1016/j.atmosenv.2020.117712, 2020c.
715 Li, X., Jiang, L., Hoa, L. P., Lyu, Y., Xu, T., Yang, X., Iinuma, Y., Chen, J., and Herrmann, H.: Size
716 distribution of particle-phase sugar and nitrophenol tracers during severe urban haze episodes in
717 Shanghai, Atmos. Environ., 145, 115-127, https://doi.org/10.1016/j.atmosenv.2016.09.030, 2016.
718 Liao, T., Wang, S., Ai, J., Gui, K., Duan, B., Zhao, Q., Zhang, X., Jiang, W., and Sun, Y.: Heavy
719 pollution episodes, transport pathways and potential sources of PM2.5 during the winter of 2013 in
720 Chengdu (China), Sci. Total Environ., 584-585, 1056-1065,
721 https://doi.org/10.1016/j.scitotenv.2017.01.160, 2017.
722 Liu, S., Wang, H., Hu, Z., Zhang, X., Sun, Y., and Dong, F.: Resolving the overlooked photochemical
723 nitrophenol transformation mechanism induced by nonradical species under visible light, P. Natl. Acad.
724 Sci. U. S. A., 121, e2401452121, doi:10.1073/pnas.2401452121, 2024.
725 Liu, T., Xu, Y., Sun, Q.-B., Xiao, H.-W., Zhu, R.-G., Li, C.-X., Li, Z.-Y., Zhang, K.-Q., Sun, C.-X.,
726 and Xiao, H.-Y.: Characteristics, Origins, and Atmospheric Processes of Amines in Fine Aerosol Particles
727 in Winter in China, J. Geophys. Res.: Atmos., 128, e2023JD038974,
728 https://doi.org/10.1029/2023JD038974, 2023a.
729 Liu, X., Wang, H., Wang, F., Lv, S., Wu, C., Zhao, Y., Zhang, S., Liu, S., Xu, X., Lei, Y., and Wang,
730 G.: Secondary Formation of Atmospheric Brown Carbon in China Haze: Implication for an Enhancing
731 Role of Ammonia, Environ. Sci. Technol., 57, 11163-11172, 10.1021/acs.est.3c03948, 2023b.
732 Liu, Y., Huang, R.-J., Lin, C., Yuan, W., Li, Y. J., Zhong, H., Yang, L., Wang, T., Huang, W., Xu, W.,
733 Huang, D. D., and Huang, C.: Nitrate-Photolysis Shortens the Lifetimes of Brown Carbon Tracers from
734 Biomass Burning, Environ. Sci. Technol., 59, 640-649, 10.1021/acs.est.4c06123, 2025.
735 Lu, C., Wang, X., Dong, S., Zhang, J., Li, J., Zhao, Y., Liang, Y., Xue, L., Xie, H., Zhang, Q., and
736 Wang, W.: Emissions of fine particulate nitrated phenols from various on-road vehicles in China, Environ.
737 Res., 179, 108709, https://doi.org/10.1016/j.envres.2019.108709, 2019.
738 Ma, Y. J., Xu, Y., Yang, T., Xiao, H. W., and Xiao, H. Y.: Measurement report: Characteristics of
739 nitrogen-containing organics in PM2.5 in Ürümqi, northwestern China – differential impacts of
740 combustion of fresh and aged biomass materials, Atmos. Chem. Phys., 24, 4331-4346, 10.5194/acp-24-

4331-2024, 2024.

Ma, Y. J., Xu, Y., Yang, T., Gui, L., Xiao, H. W., Xiao, H., and Xiao, H. Y.: The critical role of aqueous-phase processes in aromatic-derived nitrogen-containing organic aerosol formation in cities with different energy consumption patterns, Atmos. Chem. Phys., 25, 2763-2780, 10.5194/acp-25-2763-2025, 2025.

MacFarlane, S. M., Fisher, J. A., Xu, L., Wennberg, P. O., Crounse, J. D., Ball, K., Zhai, S., Bates, K. H., Kim, Y., Zhang, Q., and Blake, D. R.: Sources, Sinks, and Oxidation Pathways of Phenolic Compounds in South Korea Constrained Using KORUS-AQ Airborne Observations, J. Geophys. Res.: Atmos., 130, e2024JD043110, https://doi.org/10.1029/2024JD043110, 2025.

Mayorga, R. J., Zhao, Z., and Zhang, H.: Formation of secondary organic aerosol from nitrate radical oxidation of phenolic VOCs: Implications for nitration mechanisms and brown carbon formation, Atmos. Environ., 244, 117910, https://doi.org/10.1016/j.atmosenv.2020.117910, 2021.

Mohr, C., Lopez-Hilfiker, F. D., Zotter, P., Prévôt, A. S. H., Xu, L., Ng, N. L., Herndon, S. C., Williams, L. R., Franklin, J. P., Zahniser, M. S., Worsnop, D. R., Knighton, W. B., Aiken, A. C., Gorkowski, K. J., Dubey, M. K., Allan, J. D., and Thornton, J. A.: Contribution of Nitrated Phenols to Wood Burning Brown Carbon Light Absorption in Detling, United Kingdom during Winter Time, Environ. Sci. Technol., 47, 6316-6324, 10.1021/es400683v, 2013.

Morales, J. A., Pirela, D., de Nava, M. G., de Borrego, B. z. S., Velásquez, H., and Durán, J.: Inorganic water soluble ions in atmospheric particles over Maracaibo Lake Basin in the western region of Venezuela, Atmos. Res., 46, 307-320, https://doi.org/10.1016/S0169-8095(97)00071-9, 1998.

Nguyen, T. K. V., Zhang, Q., Jimenez, J. L., Pike, M., and Carlton, A. G.: Liquid water: ubiquitous contributor to aerosol mass, Environ. Sci. Tech. Let., 3, 257-263. https://doi.org/210.1021/acs.estlett.1026b00167, 2016.

Olariu, R. I., Klotz, B., Barnes, I., Becker, K. H., and Mocanu, R.: FT–IR study of the ring-retaining products from the reaction of OH radicals with phenol, o-, m-, and p-cresol, Atmos. Environ., 36, 3685-3697, https://doi.org/10.1016/S1352-2310(02)00202-9, 2002.

Olariu, R. I., Barnes, I., Bejan, I., Arsene, C., Vione, D., Klotz, B., and Becker, K. H.: FT-IR Product Study of the Reactions of NO3 Radicals With ortho-, meta-, and para-Cresol, Environ. Sci. Technol., 47, 7729-7738, 10.1021/es401096w, 2013.

Rana, M. S. and Guzman, M. I.: Oxidation of Catechols at the Air–Water Interface by Nitrate Radicals, Environ. Sci. Technol., 56, 15437-15448, 10.1021/acs.est.2c05640, 2022.

Salvador, C. M. G., Tang, R., Priestley, M., Li, L., Tsiligiannis, E., Le Breton, M., Zhu, W., Zeng, L., Wang, H., Yu, Y., Hu, M., Guo, S., and Hallquist, M.: Ambient nitro-aromatic compounds – biomass burning versus secondary formation in rural China, Atmos. Chem. Phys., 21, 1389-1406, 10.5194/acp-21-1389-2021, 2021.

Sareen, N., Waxman, E. M., Turpin, B. J., Volkamer, R., and Carlton, A. G.: Potential of aerosol liquid water to facilitate organic aerosol formation: assessing knowledge gaps about precursors and partitioning, Environ. Sci. Technol., 51, 3327-3335, 2017.

Selimovic, V., Yokelson, R. J., McMeeking, G. R., and Coefield, S.: Aerosol Mass and Optical Properties, Smoke Influence on O3, and High NO3 Production Rates in a Western U.S. City Impacted by Wildfires, J. Geophys. Res.: Atmos., 125, e2020JD032791, https://doi.org/10.1029/2020JD032791, 2020.

Shi, X., Qiu, X., Li, A., Jiang, X., Wei, G., Zheng, Y., Chen, Q., Chen, S., Hu, M., Rudich, Y., and Zhu, T.: Polar Nitrated Aromatic Compounds in Urban Fine Particulate Matter: A Focus on Formation via an Aqueous-Phase Radical Mechanism, Environ. Sci. Technol., 57, 5160-5168, 10.1021/acs.est.2c07324, 2023.

Vidović, K., Kroflič, A., Jovanovič, P., Šala, M., and Grgić, I.: Electrochemistry as a Tool for Studies of Complex Reaction Mechanisms: The Case of the Atmospheric Aqueous-Phase Aging of Catechols, Environ. Sci. Technol., 53, 11195-11203, 10.1021/acs.est.9b02456, 2019.

Vidović, K., Lašič Jurković, D., Šala, M., Kroflič, A., and Grgić, I.: Nighttime Aqueous-Phase Formation of Nitrocatechols in the Atmospheric Condensed Phase, Environ. Sci. Technol., 52, 9722-9730, 10.1021/acs.est.8b01161, 2018.

Wang, D., Shen, Z., Zhang, Q., Lei, Y., Zhang, T., Huang, S., Sun, J., Xu, H., and Cao, J.: Winter brown carbon over six of China's megacities: light absorption, molecular characterization, and improved source apportionment revealed by multilayer perceptron neural network, Atmos. Chem. Phys., 22, 14893-14904, 10.5194/acp-22-14893-2022, 2022.

Wang, H., Gao, Y., Wang, S., Wu, X., Liu, Y., Li, X., Huang, D., Lou, S., Wu, Z., Guo, S., Jing, S., Li, Y., Huang, C., Tyndall, G. S., Orlando, J. J., and Zhang, X.: Atmospheric Processing of Nitrophenols

799 and Nitrocresols From Biomass Burning Emissions, J. Geophys. Res.: Atmos., 125, e2020JD033401,
800 https://doi.org/10.1029/2020JD033401, 2020.
801 Wang, S. and Li, H.: NO3·-Initiated Gas-Phase Formation of Nitrated Phenolic Compounds in
802 Polluted Atmosphere, Environ. Sci. Technol., 55, 2899-2907, 10.1021/acs.est.0c08041, 2021.
803 Wang, X., Gu, R., Wang, L., Xu, W., Zhang, Y., Chen, B., Li, W., Xue, L., Chen, J., and Wang, W.:
804 Emissions of fine particulate nitrated phenols from the burning of five common types of biomass,
805 Environ. Pollut., 230, 405-412, https://doi.org/10.1016/j.envpol.2017.06.072, 2017.
806 Wang, Y., Zhao, Y., Wang, Y., Yu, J. Z., Shao, J., Liu, P., Zhu, W., Cheng, Z., Li, Z., Yan, N., and
807 Xiao, H.: Organosulfates in atmospheric aerosols in Shanghai, China: seasonal and interannual variability,
808 origin, and formation mechanisms, Atmos. Chem. Phys., 21, 2959-2980, 10.5194/acp-21-2959-2021,
809 2021.
810 Wang, Y., Hu, M., Wang, Y., Zheng, J., Shang, D., Yang, Y., Liu, Y., Li, X., Tang, R., Zhu, W., Du,
811 Z., Wu, Y., Guo, S., Wu, Z., Lou, S., Hallquist, M., and Yu, J. Z.: The formation of nitro-aromatic
812 compounds under high NOx and anthropogenic VOC conditions in urban Beijing, China, Atmos. Chem.
813 Phys., 19, 7649-7665, 10.5194/acp-19-7649-2019, 2019.
814 Xie, M., Chen, X., Hays, M. D., and Holder, A. L.: Composition and light absorption of N-
815 containing aromatic compounds in organic aerosols from laboratory biomass burning, Atmos. Chem.
816 Phys., 19, 2899-2915, 10.5194/acp-19-2899-2019, 2019.
817 Xiong, H., Liu, X., Sun, C., Zhang, X., Wang, X., Lin, J., Xue, L., Sun, X., Shang, X., Ma, F., Xie,
818 H., Chen, J., Yan, G., Shu, J., Fu, H., Wang, L., Rudich, Y., George, C., Mellouki, A., Zhao, D., Wang,
819 X., Herrmann, H., and Chen, J.: Atmospheric water cluster–catalyzed formation of nitroaromatics as a
820 secondary aerosol source, Sci. Adv., 11, eadv7805, doi:10.1126/sciadv.adv7805, 2025.
821 Xu, Y., Xiao, H., Wu, D., and Long, C.: Abiotic and Biological Degradation of Atmospheric
822 Proteinaceous Matter Can Contribute Significantly to Dissolved Amino Acids in Wet Deposition,
823 Environ. Sci. Technol., 54, 6551-6561. https://doi.org/6510.1021/acs.est.6550c00421, 2020a.
824 Xu, Y., Dong, X.-N., Xiao, H.-Y., Zhou, J.-X., and Wu, D.-S.: Proteinaceous Matter and Liquid
825 Water in Fine Aerosols in Nanchang, Eastern China: Seasonal Variations, Sources, and Potential
826 Connections, J. Geophys. Res.: Atmos., 127, e2022JD036589.
827 https://doi.org/036510.031029/032022JD036589, 2022.

Xu, Y., Dong, X. N., He, C., Wu, D. S., Xiao, H. W., and Xiao, H. Y.: Mist cannon trucks can exacerbate the formation of water-soluble organic aerosol and PM2.5 pollution in the road environment, Atmos. Chem. Phys., 23, 6775-6788, 10.5194/acp-23-6775-2023, 2023.

Xu, Y., Lin, X., Sun, Q.-B., Xiao, H.-W., Xiao, H., and Xiao, H.-Y.: Elaborating the Atmospheric Transformation of Combined and Free Amino Acids From the Perspective of Observational Studies, J. Geophys. Res.: Atmos., 129, e2024JD040730. https://doi.org/040710.041029/042024JD040730, https://doi.org/10.1029/2024JD040730, 2024a.

Xu, Y., Liu, T., Ma, Y. J., Sun, Q. B., Xiao, H. W., Xiao, H., Xiao, H. Y., and Liu, C. Q.: Measurement report: Occurrence of aminiums in PM2.5 during winter in China – aminium outbreak during polluted episodes and potential constraints, Atmos. Chem. Phys., 24, 10531-10542, 10.5194/acp-24-10531-2024, 2024b.

Xu, Y., Ma, Y. J., Yang, T., Sun, Q. B., Wang, Y. C., Gui, L., Xiao, H. W., Xiao, H., and Xiao, H. Y.: Molecular evidence on potential contribution of marine emissions to aromatic and aliphatic organic sulfur and nitrogen aerosols in the South China Sea, Atmos. Chem. Phys., 25, 13621-13634, 10.5194/acp-25-13621-2025, 2025.

Xu, Y., Miyazaki, Y., Tachibana, E., Sato, K., Ramasamy, S., Mochizuki, T., Sadanaga, Y., Nakashima, Y., Sakamoto, Y., Matsuda, K., and Kajii, Y.: Aerosol Liquid Water Promotes the Formation of Water-Soluble Organic Nitrogen in Submicrometer Aerosols in a Suburban Forest, Environ. Sci. Technol., 54, 1406-1414. https://doi.org/1410.1021/acs.est.1409b05849, 2020b.

Yang, T., Xu, Y., Wang, Y. C., Ma, Y. J., Xiao, H. W., Xiao, H., and Xiao, H. Y.: Non-biogenic sources are an important but overlooked contributor to aerosol isoprene-derived organosulfates during winter in northern China, Atmos. Chem. Phys., 25, 2967-2978, 10.5194/acp-25-2967-2025, 2025.

Yang, T., Xu, Y., Ma, Y.-J., Wang, Y.-C., Yu, J. Z., Sun, Q.-B., Xiao, H.-W., Xiao, H.-Y., and Liu, C.-Q.: Field Evidence for Constraints of Nearly Dry and Weakly Acidic Aerosol Conditions on the Formation of Organosulfates, Environ. Sci. Technol. Lett., 11, 981-987, 10.1021/acs.estlett.4c00522, 2024.

Yang, T., Xu, Y., Ye, Q., Ma, Y. J., Wang, Y. C., Yu, J. Z., Duan, Y. S., Li, C. X., Xiao, H. W., Li, Z. Y., Zhao, Y., and Xiao, H. Y.: Spatial and diurnal variations of aerosol organosulfates in summertime Shanghai, China: potential influence of photochemical processes and anthropogenic sulfate pollution,

Atmos. Chem. Phys., 23, 13433-13450, 10.5194/acp-23-13433-2023, 2023.

Yang, W., You, D., Li, C., Han, C., Tang, N., Yang, H., and Xue, X.: Photolysis of Nitroaromatic Compounds under Sunlight: A Possible Daytime Photochemical Source of Nitrous Acid?, Environ. Sci. Technol. Lett., 8, 747-752, 10.1021/acs.estlett.1c00614, 2021.

Yang, Y., Li, X., Shen, R., Liu, Z., Ji, D., and Wang, Y.: Seasonal variation and sources of derivatized phenols in atmospheric fine particulate matter in North China Plain, J. Environ. Sci., 89, 136-144, https://doi.org/10.1016/j.jes.2019.10.015, 2020.

Yin, M.-J., Xu, Y., Zhu, R.-G., Wang, Y., Sun, Q.-B., Gui, L., You, Y.-C., Tao, J.-L., Xiao, H.-W., Xiao, H., and Xiao, H.-Y.: Field New Insights into Bioaerosol Amino Acid Origin and Atmospheric Degradation: Significant Dust Contribution and Drying Effect, Environ. Sci. Technol., 60, 688-699, 10.1021/acs.est.5c12980, 2026.

You, Y.-C., Yang, T., Xu, Y., Gui, L., Wang, Y.-C., Yin, M.-J., Xiao, H., Xiao, H.-W., and Xiao, H.-Y.: Novel Discoveries about the Potential Nonsecondary Origins of C2–C3 Organosulfates in Ambient Aerosol Particles, Environ. Sci. Technol., 60, 6298-6309, 10.1021/acs.est.5c18511, 2026.

Zhang, B., Shen, Z., He, K., Sun, J., Huang, S., Xu, H., Li, J., Ho, S. S. H., and Cao, J.-j.: Insight into the Primary and Secondary Particle-Bound Methoxyphenols and Nitroaromatic Compound Emissions from Solid Fuel Combustion and the Updated Source Tracers, Environ. Sci. Technol., 57, 14280-14288, 10.1021/acs.est.3c04370, 2023.

Zhang, Y.-L. and Cao, F.: Fine particulate matter (PM2.5) in China at a city level, Sci. Rep., 5, 14884, 10.1038/srep14884, 2015.